Journal of Hydrology 568 (2019) 758–768

Contents lists available at ScienceDirect

Journal of Hydrology

journal homepage: www.elsevier.com/locate/jhydrol

Research papers

Identifying time-varying hydrological model parameters to improve simulation efficiency by the ensemble Kalman filter: A joint assimilation of streamflow and actual evapotranspiration

Mengsi Xiong[a,b], Pan Liu[a,b,*], Lei Cheng[a,b], Chao Deng[c,d], Ziling Gui[a,b], Xiaojing Zhang[a,b], Yanghe Liu[a,b]

[a] State Key Laboratory of Water Resources and Hydropower Engineering Science, Wuhan University, Wuhan 430072, China
[b] Hubei Provincial Collaborative Innovation Center for Water Resources Security, Wuhan 430072, China
[c] State Key Laboratory of Hydrology-Water Resources and Hydraulic Engineering, Hohai University, Nanjing 210098, China
[d] College of Water Resources and Hydrology, Hohai University, Nanjing 210098, China

ARTICLE INFO

This manuscript was handled by Marco Borga, Editor-in-Chief, with the assistance of Hamid Moradkhani, Associate Editor

Keywords:
Multivariate data assimilation
Time-varying model parameter
Ensemble Kalman filter

ABSTRACT

Hydrological model parameters are essential for model simulation, which may vary with time owing to climatic variations and human activities. As a result, the implementation of stationary parameters may lead to inaccurate streamflow simulation. Actual evapotranspiration (*ET*) is a crucial component of hydrological cycles with an important influence on regional climate characteristics. Our aim was to investigate an appropriate way to estimate time-varying parameters using streamflow and *ET* observations, and to explore the how the simulation efficiency would change when *ET* data were added into assimilation. Data assimilation techniques can automatically adjust hydrological model parameters according to changing conditions. The ensemble Kalman filter (EnKF) technique was used to assimilate observations into a two-parameter monthly water balance model. Four data assimilation schemes were designed and applied in a synthetic experiment and 173 catchments in USA, including: (1) sole assimilation of streamflow to update both parameters, (2) joint assimilation of streamflow and *ET* to simultaneously update parameters, (3) sole assimilation of *ET* first to update parameter *C* (measuring evapotranspiration), and then subsequently joint assimilation of streamflow and *ET* to update parameter *SC* (measuring water storage capacity), and (4) sole assimilation of *ET* to update parameter *C*, and then sole assimilation of streamflow to update parameter *SC*. The four schemes were compared in terms of deterministic and probabilistic model performances, and model parameter correlations. The results indicated that: (1) the estimation of parameter *C* can be improved by assimilating *ET* observations into the model, and the time-varying model parameters obtained by adding *ET* data into assimilation led to a significant enhancement in deterministic streamflow and *ET* prediction, (2) among the three joint assimilation schemes, the deterministic model simulation performances were similar, while the ensemble predictions were more reliable in scheme 2. The joint assimilation of streamflow and *ET* to update both parameters in one step, i.e., scheme 2, outperformed the other two schemes in parameter *SC* estimation and model performance, (3) the ability to enhance simulation accuracy and to weaken correlations between parameters was more significant in humid catchments. The joint assimilation was helpful for the application of multiple sources of information into a hydrological simulation.

1. Introduction

Hydrological model parameters play a critical role in model simulation. It is generally assumed that model parameters calibrated by limited data will be applicable in the future. In other words, the parameters of hydrological models are treated as constants while model inputs are vary over time. However, this assumption may lead to large errors in simulated streamflow owing to climatic temporal variations and human activities. There is an increasing awareness of the need to consider model parameters as continuously time-varying (Brigode et al., 2013; Thirel et al., 2015; Patil and Stieglitz, 2015). On one hand, model parameters may potentially vary with climatic temporal variations because calibrated parameters are supposed to compensate for model structure and observation data problems (Wagener et al., 2003;

* Corresponding author at: State Key Laboratory of Water Resources and Hydropower Engineering Science, Wuhan University, Wuhan 430072, China.
E-mail address: liupan@whu.edu.cn (P. Liu).

https://doi.org/10.1016/j.jhydrol.2018.11.038
Received 4 December 2017; Received in revised form 8 November 2018; Accepted 13 November 2018
Available online 17 November 2018

Merz et al., 2011). On the other hand, human activities, such as the construction of water conservancy projects and urbanization, could result in underlying surface changes, which also may change model parameters because some parameters represent transient catchment characteristics (Legesse et al., 2003; Brown et al., 2005). Hence, it is of paramount importance to study the time-variability of hydrological model parameters.

Several approaches have been used to obtain time-varying model parameters in response to climatic temporal variations and human activities (Deng et al., 2016). One is to establish the functional form of the selected time-varying model parameters (e.g., Marshall et al., 2006; Jeremiah et al., 2013). Westra et al. (2014) proposed a strategy for diagnosing and interpreting hydrological model non-stationarity by assuming parameters vary in time as functions of seasonality, annual variability and longer-term trends. Another is to divide the data into several consecutive subsets and calibrate the model parameters in each subset based on optimization algorithms (e.g., Seibert et al., 2010; de Vos et al., 2010; Gharari et al., 2013; Vaze et al., 2010). Merz et al. (2011) calibrated the parameters of a conceptual rainfall-runoff model in six consecutive 5-year periods between 1976 and 2006 for 273 catchments in Austria to analyze the temporal changes in model parameters. A common shortcoming with these approaches is that scientific judgement is still required to estimate what the identified parameter trends might be, and modelers may need to adjust the model framework according to different situations (Pathiraja et al., 2016a).

Data Assimilation (DA) method can adjust hydrological model parameters automatically according to changing conditions. The basic idea of DA is to quantify errors in both the hydrological model and observations, and combine model simulations with observations optimally to update hydrological model states (Clark et al., 2008). DA has been used to update model states and model parameters simultaneously in real time with the advanced simulation capability of streamflow better than in most other optimization algorithms (e.g., Moradkhani et al., 2005; Wang et al., 2009; Pathiraja et al., 2017; Abbaszadeh et al., 2018). Only a minority of studies have focused on generating time-varying parameters with DA (e.g., Smith et al., 2008; Moradkhani et al., 2012; Vrugt et al., 2013; Pathiraja et al., 2016b; Feng et al., 2017; Pathiraja et al., 2018). Applications of DA can be classified into univariate and multivariate assimilations according to the assimilated data (Montzka et al., 2012). Univariate assimilation using a single observation data type (e.g. streamflow) accounts for most data assimilation applications. Multivariate or joint assimilation refers to the use of more than one data type (e.g. streamflow and soil moisture). Most studies have concluded that the results obtained from multivariate assimilation are better than from univariate assimilation (e.g., Camporese et al., 2009; Shi et al., 2015). Yan and Moradkhani (2016) compared the joint and separate assimilation of streamflow and satellite soil moisture into the Sacramento soil moisture accounting model and found that solely assimilating streamflow could lead to inaccurate soil moisture estimation.

Actual evapotranspiration (*ET*) is a crucial component of hydrological cycles with an important influence on regional climate characteristics (Jung et al., 2010). Several researchers have applied data assimilation techniques to assimilate *ET* data into hydrological models (e.g., Schuurmans et al., 2003; Kalma et al., 2008; Dong et al., 2016). Qin et al. (2008) assimilated remotely sensed *ET* into a distributed hydrological model and found that this improved the predictions of spatial water distribution over a large river basin. Zou et al., 2017 proposed a catchment scale *ET* data assimilation technique that assimilated remotely sensed *ET* data into a distributed time-variant gain hydrological model and found that assimilating *ET* into hydrological models led to improved predictions of soil moisture and streamflow. However, the current research on the assimilation of *ET* data mainly focuses on estimation of *ET*, and has not addressed the impact on time-varying parameters.

The purpose of this study was to investigate an appropriate way to estimate time-varying parameters using streamflow and *ET* observations, and to explore how the simulation efficiency would change when *ET* data were added into assimilation. The ensemble Kalman filter (EnKF) method was used to assimilate streamflow and *ET* into the hydrological model. This paper is organized as follows: Section 2 describes the hydrological model, the EnKF method and our experimental design. Section 3 illustrates the case study, including the synthetic experiment, the study area and parameter setting. Results and discussion are presented in Section 4, then we conclude with a summary of the main outcomes in Section 5.

2. Methodology

2.1. Monthly water balance model

The two-parameter monthly water balance model developed by Xiong and Guo (1999) has been widely used in monthly runoff simulation because the model is simple and has a high simulation accuracy (e.g., Guo et al., 2002; Xiong and Guo, 2012). The inputs of the model are monthly potential evapotranspiration (*PET*) and monthly areal precipitation (*P*), and the outputs include monthly runoff (*Q*) and *ET*. *ET* is calculated using the following formula:

$$E_t = C \times EP_t \times \tanh(P_t/EP_t) \quad (1)$$

where E_t is the actual monthly evapotranspiration, P_t is the monthly rainfall, EP_t represents the monthly potential evapotranspiration value, and C is the first model parameter in the monthly water balance model which comprehensively reflects the variation of precipitation and evapotranspiration (Table 1).

The monthly runoff has close relationship with the soil water content (*S*) and is calculated as follows:

$$Q_t = S_t \times \tanh(S_t/SC) \quad (2)$$

where Q_t is the monthly runoff, S_t is the soil water content, and SC is the second model parameter in the monthly water balance model which is used to represent the water storage capacity of catchments (Table 1). The quantity of the remaining water in the soil at the *t*-th month is computed by $S_{t-1} + P_t - E_t$. Next, the monthly runoff is calculated as follows:

$$Q_t = (S_{t-1} + P_t - E_t) \times \tanh[(S_{t-1} + P_t - E_t)/SC] \quad (3)$$

Finally, the soil water content at the end of the *t*-th month is calculated according to the water conservation law:

$$S_t = S_{t-1} + P_t - E_t - Q_t \quad (4)$$

2.2. Ensemble Kalman filter

The EnKF is a sequential data assimilation technique, using the Monte-Carlo method to approximate error covariance matrix. This is done by generating an ensemble of state simulations to update the state variables and model parameters, conditioned on a series of observations (Evensen, 1994; Deng et al., 2015). An effective method for implementing the EnKF is as follows:

(1) Initialize. Set the ensemble size N and the total length of assimilation time steps n. At the first time step, the state variable ensembles are generated by a Gaussian distribution.

Table 1
Description and prior ranges of the two parameters for the monthly water balance model.

Parameters	Description	Interval and unit
C	Evapotranspiration parameter	0.2–2.0 (–)
SC	Water storage capacity	100–2000 (mm)

(2) Forecast. Initialize the background field with the analysis of state variables at time step k. Then generate the forecast of model parameters and state variables by perturbing the updated values from the previous time step. The state equation is as follows:

$$\begin{pmatrix}\theta_{i,k+1}^{f}\\ x_{i,k+1}^{f}\end{pmatrix}=\begin{pmatrix}\theta_{i,k}^{a}\\ f(x_{i,k}^{a},\ \theta_{i,k+1}^{f},\ u_{k+1})\end{pmatrix}+\begin{pmatrix}\delta_{i,k}\\ \varepsilon_{i,k}\end{pmatrix},\ \ \delta_{i,k}\tilde{\mathrm{N}}(0,\ R_k),\ \varepsilon_{i,k}\tilde{\mathrm{N}}(0,\ G_k) \tag{5}$$

where θ_i is the parameter vector and x_i is the state vector; $\theta_{i,k+1}^{f}$ and $x_{i,k+1}^{f}$ are the i-th ensemble member forecast at time step $k+1$; $\theta_{i,k}^{a}$ and $x_{i,k}^{a}$ are the analysis of the i-th ensemble member at time step k; f is the forward operator. u_{k+1} is the forcing data (e.g. precipitation) at time step $k+1$; $\delta_{i,k}$ and $\varepsilon_{i,k}$ are the white noise for the i-th ensemble member. It should be noted that the model error is displayed by $\varepsilon_{i,k}$ and represents all the uncertainties related to model structure and the forcing data.

(3) Perturb observations.

$$y_{k+1}=h(x_{k+1},\ \theta_{k+1})+\xi_{k+1},\ \ \xi_{k+1}\tilde{\mathrm{N}}(0,\ S_k) \tag{6}$$

$$y_{i,k+1}=y_{k+1}+\xi_{i,k+1} \tag{7}$$

Eq. (6) is the observation equation, where y_{k+1} is the observation vector at time $k+1$; h is the observational operator that converts the model states to observations; ξ_{k+1} is the measurement error that follows Gaussian distribution; $y_{i,k+1}$ is the i-th observations ensemble member at time step $k+1$;

(4) Update. With the observations being available, the updating process of model parameters and state variables can be formalized as follows:

$$\begin{pmatrix}x_{i,k+1}^{a}\\ \theta_{i,k+1}^{a}\end{pmatrix}=\begin{pmatrix}x_{i,k+1}^{f}\\ \theta_{i,k+1}^{f}\end{pmatrix}+\begin{pmatrix}K_{k+1}^{x}[y_{i,k+1}-h(x_{i,k+1}^{f},\ \theta_{i,k+1}^{f})]\\ K_{k+1}^{\theta}[y_{i,k+1}-h(x_{i,k+1}^{f},\ \theta_{i,k+1}^{f})]\end{pmatrix} \tag{8}$$

where K_{k+1} is the Kalman gain matrix, which can be calculated by the following equations (Moradkhani et al., 2005):

$$K_{k+1}^{x}=\sum_{k+1}^{xy}\left(\sum_{k+1}^{yy}+S_k\right)^{-1} \tag{9}$$

$$K_{k+1}^{\theta}=\sum_{k+1}^{\theta y}\left(\sum_{k+1}^{yy}+S_k\right)^{-1} \tag{10}$$

$$\sum_{k+1}^{xy}=\frac{1}{N-1}\sum_{i=1}^{N}(x_{i,k+1}^{f}-\bar{x}_{k+1}^{f})(\hat{y}_{i,k+1}-\hat{y}_{i,k+1}^{m})^{T} \tag{11}$$

$$\sum_{k+1}^{\theta y}=\frac{1}{N-1}\sum_{i=1}^{N}(\theta_{i,k+1}^{f}-\bar{\theta}_{k+1}^{f})(\hat{y}_{i,k+1}-\hat{y}_{i,k+1}^{m})^{T} \tag{12}$$

$$\sum_{k+1}^{yy}=\frac{1}{N-1}\sum_{i=1}^{N}(\hat{y}_{i,k+1}-\hat{y}_{i,k+1}^{m})(\hat{y}_{i,k+1}-\hat{y}_{i,k+1}^{m})^{T} \tag{13}$$

where $\sum_{k+1}^{xy}$ is the cross covariance of the forecasted states $x_{i,k+1}^{f}$ and simulated $\hat{y}_{i,k+1}$ (Snyder and Zhang, 2003); $\sum_{k+1}^{\theta y}$ is the cross covariance of the forecasted parameters and simulated $\hat{y}_{i,k+1}$; $\sum_{k+1}^{yy}$ is the error covariance of the simulated $\hat{y}_{i,k+1}$ (Mitchell and Houtekamer, 2000); $\bar{x}_{k+1}^{f}$ and $\bar{\theta}_{k+1}^{f}$ are the ensemble mean of the forecasted states and parameters, respectively; $\hat{y}_{i,k+1}^{m}$ is the ensemble mean of the simulated $\hat{y}_{i,k+1}$.

2.3. Experimental design

Based on the two-parameter monthly water balance model, the state and observation equations are as follows:

State equations:

$$\begin{pmatrix}C_{i,k+1}^{f}\\ SC_{i,k+1}^{f}\\ S_{i,k+1}^{f}\end{pmatrix}=\begin{pmatrix}C_{i,k}^{a}\\ SC_{i,k}^{a}\\ f(S_{i,k}^{a},\ C_{i,k+1}^{f},\ SC_{i,k+1}^{f})\end{pmatrix}+\begin{pmatrix}\delta_{1,i,k}\\ \delta_{2,i,k}\\ \varepsilon_{i,k}\end{pmatrix} \tag{14}$$

$$(C_{i,k+1}^{f})=(C_{i,k}^{a})+(\delta_{1,i,k}) \tag{15}$$

$$\begin{pmatrix}SC_{i,k+1}^{f}\\ S_{i,k+1}^{f}\end{pmatrix}=\begin{pmatrix}SC_{i,k}^{a}\\ f(S_{i,k}^{a},\ C_{i,k+1}^{f},\ SC_{i,k+1}^{f})\end{pmatrix}+\begin{pmatrix}\delta_{2,i,k}\\ \varepsilon_{2,i,k}\end{pmatrix} \tag{16}$$

Observation equations:

$$Q_{k+1}=h(S_{k+1}^{f},\ C_{k+1}^{f},\ SC_{k+1}^{f})+\xi_{1,k+1} \tag{17}$$

$$ET_{k+1}=h(C_{k+1}^{f})+\xi_{2,k+1} \tag{18}$$

$$\begin{pmatrix}Q_{k+1}\\ ET_{k+1}\end{pmatrix}=\begin{pmatrix}h(S_{k+1}^{f},\ C_{k+1}^{f},\ SC_{k+1}^{f})\\ h(C_{k+1}^{f})\end{pmatrix}+\begin{pmatrix}\xi_{1,k+1}\\ \xi_{2,k+1}\end{pmatrix} \tag{19}$$

Four schemes were designed to generate time-varying model parameters by univariate and multivariate assimilation methods.

Scheme 1 updates the model parameters C and SC by only assimilating the streamflow data, with the state variable being S, which is set by a comparative experiment. Besides, ET had also been solely assimilated into the hydrological model, while the streamflow simulation accuracy decreases ($NSE < 0$). Thus, only sole streamflow assimilation is discussed here. Scheme 1 includes Eqs. (14) and (17).

Scheme 2 is joint assimilation, updating the state variable S, and model parameters C and SC simultaneously by assimilating streamflow and ET. Scheme 2 includes Eqs. (14) and (19).

It is shown in Eqs. (1)–(4) that C is used to estimate ET, while SC has relationship with both streamflow and ET. Therefore, schemes 3 and 4 were designed to investigate whether the different assimilation steps of the model parameters in the joint assimilation of Q and ET had any influence on the parameter estimations and model simulations. Scheme 3 updates the model parameter C by solely assimilating ET first, then updates SC and the state variable S by jointly assimilating streamflow and ET, using the ensemble average of C from the previous step to calculate E_t in Eqs. (3) and (4). The first step of scheme 3 includes Eqs. (15) and (18), and the update of SC includes Eqs. (16) and (19). It should be noted that the state variable S will have correlated errors with ET observations, because ET observations have been used to update C in the first step and C is used to generate a forecast of S. Here scheme 3 is set as an alternative scheme to assimilate ET data into the hydrological model.

Scheme 4 is a comparative experiment based on scheme 3. The difference between them is the update of SC, scheme 3 uses streamflow and ET observations while scheme 4 uses the streamflow information only. The update of C includes Eqs. (15) and (18), and the update of SC includes Eqs. (16) and (17).

2.4. Evaluation index

The Nash-Sutcliffe efficiency coefficient (NSE) (Nash and Sutcliffe, 1970) is used as an indicator of deterministic model performance in evaluating the simulation of streamflow and ET:

$$NSE=1-\frac{\sum_{i=1}^{n}(Q_{sim,i}-Q_{obs,i})^2}{\sum_{i=1}^{n}(Q_{obs,i}-\bar{Q}_{obs})^2} \tag{20}$$

where $Q_{obs,i}$ and $Q_{sim,i}$ are the observed and simulated runoff for month i; $\bar{Q}_{obs}$ is the mean value of observed runoff; n is the total number of data points. NSE ranges from $-\infty$ to 1. An NSE value of 1 means a perfect match of simulated runoff to the observations.

In terms of probabilistic performance measures, the 95% exceedance ratio ($ER95$) (DeChant and Moradkhani, 2012) and reliability

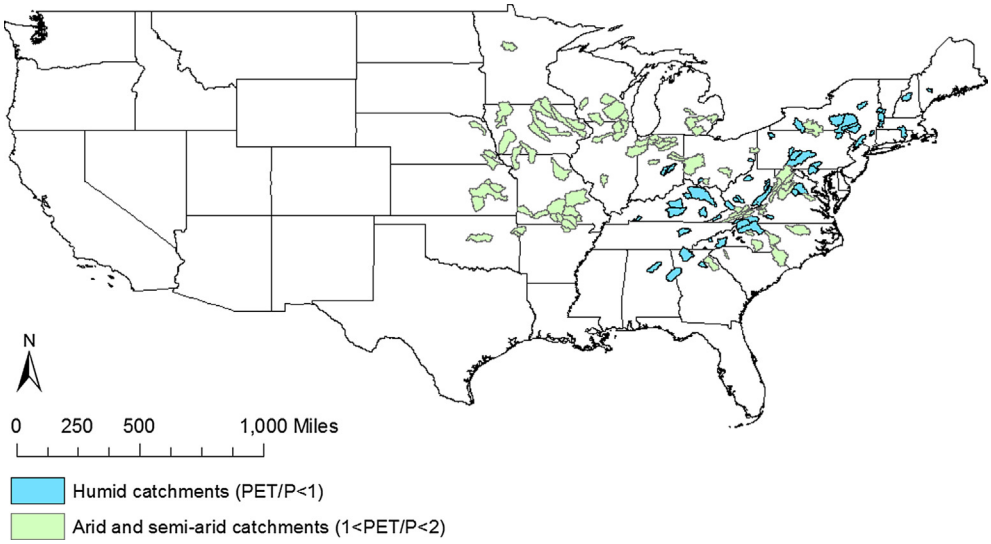

Fig. 1. Location of the catchments and classification into humid catchments (blue) and arid and semi-arid catchments (green). (For interpretation of the references to colour in this figure legend, the reader is referred to the web version of this article.)

the optimal values at intervals of 0.01 from 0 to 0.2.

4. Results and discussion

4.1. Synthetic experiment

To assess the performance of the four assimilation schemes, the comparisons of the assimilated and true model parameters under different scenarios are presented in Fig. 3. Table 3 shows the evaluation statistics for parameters, streamflow and *ET*. Fig. 3 shows that the assimilated parameters of *C* and *SC* had similar trends to the true parameters, and the estimation of *C* in schemes 2, 3 and 4 matched the true values more closely when the *ET* observations were added into the assimilation. It should be noted that there was a time lag between the assimilated *C* and the true values, because of the defect in the EnKF technique. In the EnKF, the state and parameters are updated based on

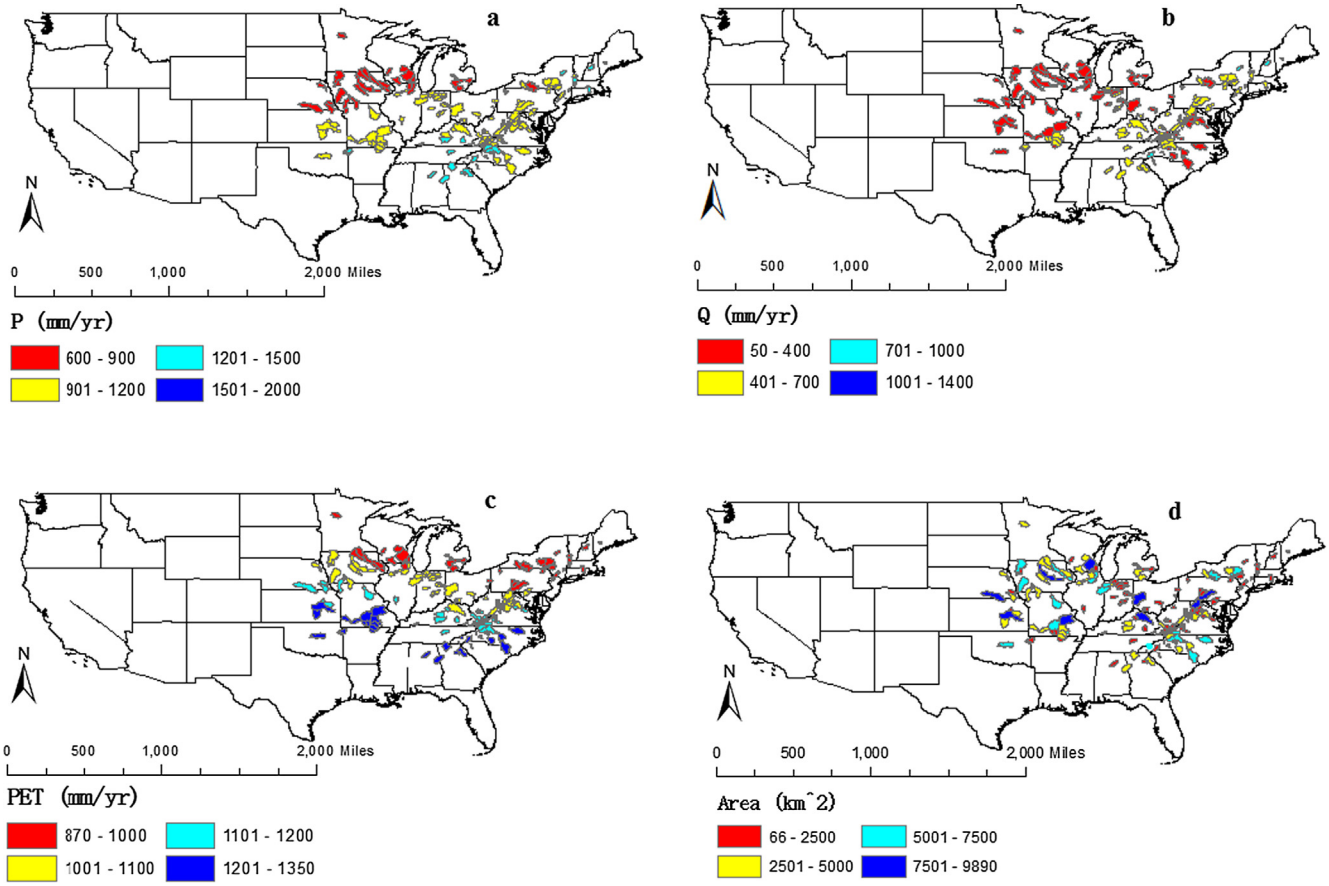

Fig. 2. Annual mean values of climatic variables and areas for the 173 catchments.

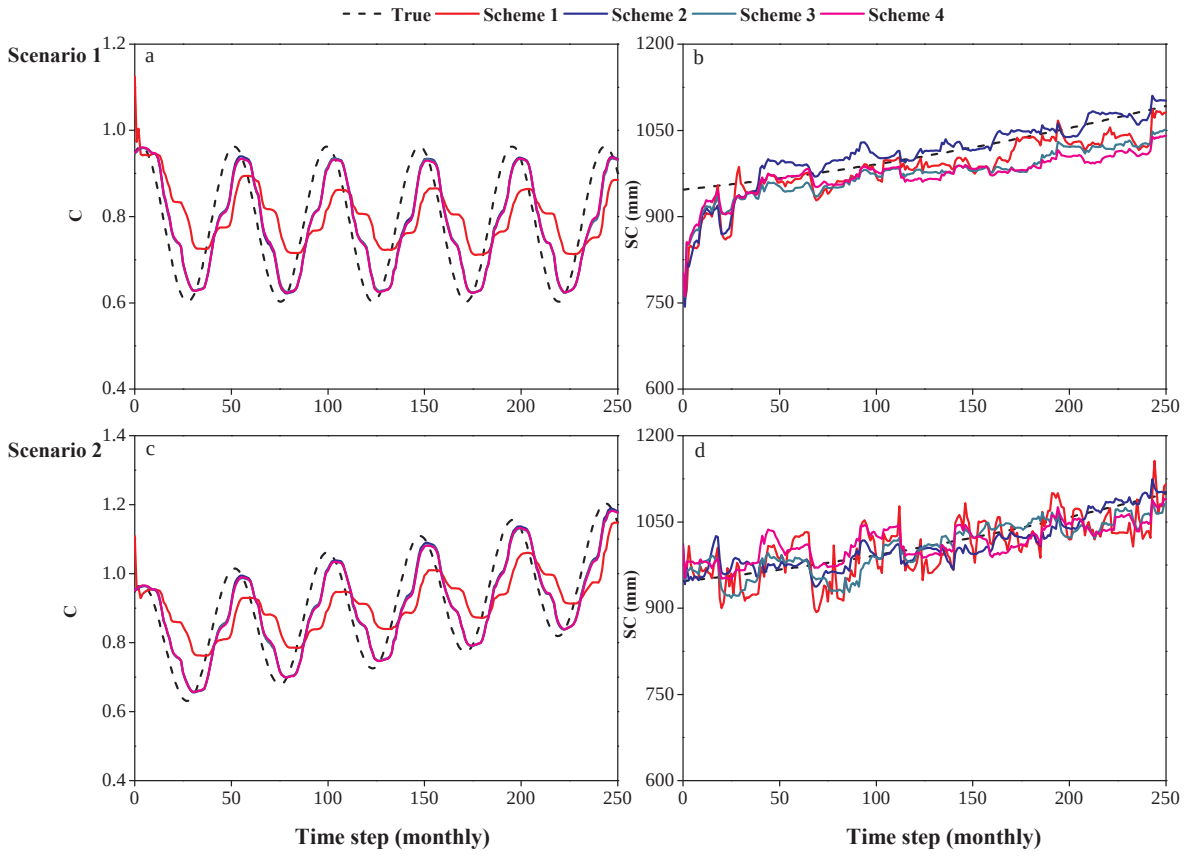

Fig. 3. Model parameters (evapotranspiration parameter *C*, water storage capacity *SC*) of true (dashed line) and assimilated (solid lines) values for scheme 1 (red), scheme 2 (blue), scheme 3 (green) and scheme 4 (magenta) under different scenarios in the synthetic experiment. (For interpretation of the references to colour in this figure legend, the reader is referred to the web version of this article.)

Table 3
Performance statistics for parameters, streamflow and *ET* estimation in the synthetic experiment.

Schemes	Parameter *C*			Parameter *SC*			Streamflow			*ET*
	RMSE	*MARE*	*R*	*RMSE*	*MARE*	*R*	NSE_Q	ER95 (%)	*α*	NSE_{ET}
	(1) Scenario 1									
Scheme 1	0.12	0.136	0.44	39.13	0.027	0.84	0.997	5.6	0.96	0.938
Scheme 2	0.07	0.077	0.85	33.17	0.021	0.86	0.999	5.2	0.94	0.984
Scheme 3	0.07	0.078	0.84	41.25	0.036	0.89	0.998	5.6	0.69	0.983
Scheme 4	0.07	0.078	0.84	45.52	0.037	0.80	0.999	5.6	0.69	0.983
	(2) Scenario 2									
Scheme 1	0.12	0.117	0.61	36.54	0.031	0.71	0.998	6.7	0.93	0.954
Scheme 2	0.06	0.061	0.91	18.76	0.014	0.91	0.999	6.0	0.93	0.989
Scheme 3	0.07	0.067	0.89	23.64	0.019	0.87	0.997	7.2	0.56	0.989
Scheme 4	0.07	0.066	0.89	28.78	0.024	0.77	0.999	6.8	0.55	0.988

the current observations and previous forecasts, and there may be a time lag when the EnKF method is adopted to estimate the model parameters and observations (Clark et al., 2008). Table 3 also shows that the *SC* assimilation performed the best in scheme 2. The deterministic measure (*NSE*) of streamflow and *ET* showed that the estimation of streamflow using the EnKF method very closely matched the observations with NSE_Q values of over 0.99, and the simulations of *ET* were more accurate in schemes 2, 3 and 4. In terms of the probabilistic performance, the ER95 values were between 5% and 8% for all four schemes, demonstrated that the all four schemes could produce accurate 95% predictive bounds. The reliability results suggested that the ensemble predictions were more reliable in schemes 1 and 2, with reliability indexes *α* over 0.9. The reliability indexes of schemes 3 and 4 were around 0.6, and the *p* values showed that schemes 3 and 4 tended to underpredict the high flows.

The above results demonstrated that the time-varying model parameter estimation framework using the EnKF method was able to identify the temporal variation of the model parameters, and to produce accurate 95% predictive bounds for streamflow. The estimation of parameter *C* (measuring evapotranspiration) can be improved by assimilating *ET* observations into the model. For the three joint assimilation schemes, the deterministic model performances were similar, while the ensemble predictions were more reliable in scheme 2. The joint assimilation of streamflow and *ET* to update both parameters in one step, i.e., scheme 2, outperformed the other two in parameter *SC* estimation and reliable ensemble prediction.

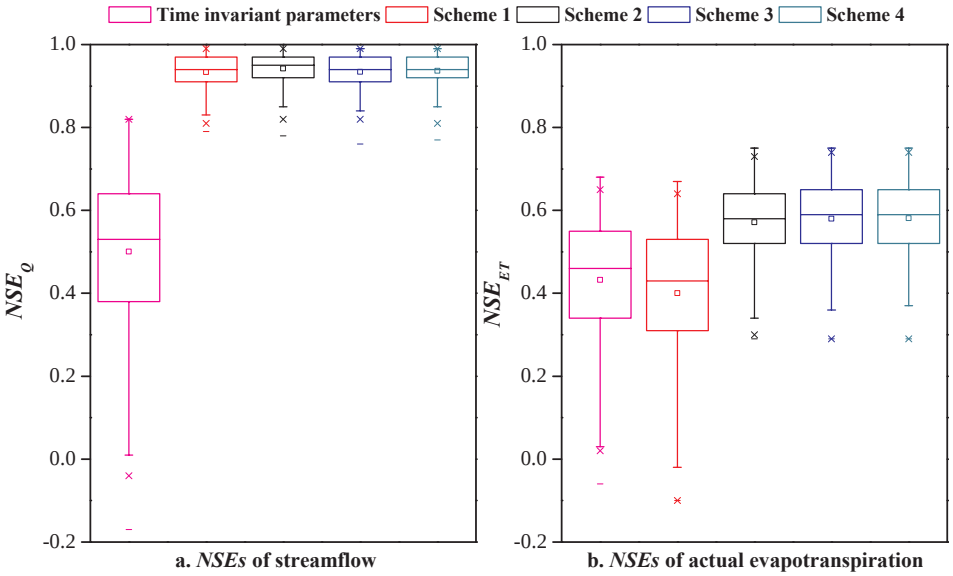

Fig. 4. The Nash-Sutcliffe efficiency coefficients of streamflow and actual evapotranspiration for time invariant parameters (magenta box), scheme 1 (red box), scheme 2 (black box), scheme 3 (blue box) and scheme 4 (green box). The box-whisker plots show the minimum, maximum, median, mean, lower quartile and upper quartile of the 173 catchments. (For interpretation of the references to colour in this figure legend, the reader is referred to the web version of this article.)

4.2. Model performance with time-varying parameters

It is of interest to understand the impact of time-varying model parameters generated from different assimilation schemes on the hydrological simulation. A no assimilation experiment that used the SCE-UA method to calibrate the time invariant model parameters was compared with the four assimilation schemes. Fig. 4 shows the *NSEs* of streamflow (NSE_Q) and *ET* (NSE_{ET}). The *NSEs* in the assimilation schemes were calculated based on the states after the analysis step of the EnKF. Fig. 5 shows the *NSEs* in the assimilation schemes before the analysis step of the EnKF. As shown in Figs. 4 and 5, the NSE_S of schemes 3 and 4 were similar to the NSE_S of scheme 2, confirming the results found in the synthetic experiment. Therefore, only schemes 1 and 2 and time invariant parameters scheme were further discussed.

The difference values of *NSE* between schemes 1–2 and the time invariant parameters scheme are shown in Fig. 6 (a positive value indicates that the performance of the time-varying parameter scheme is better). For scheme 1, the streamflow simulations for 65% of the catchments were better with the time-varying parameters than for the time invariant parameters (see Fig. 6a, the forecast NSE_Q values were higher in 98 catchments and the same in 15 catchments), and the simulation for the actual evaporation was worse in most catchments (see Fig. 6c), perhaps because the estimations for parameter *C* from scheme 1 were poor. For scheme 2, the streamflow simulations for 86% of the catchments were better than those based on the time invariant parameters (see Fig. 6b, the forecast NSE_Q values were higher in 139 catchments and the same in 9 catchments), and significant improvement of *ET* simulation accuracy can be observed (see Fig. 6d). The results indicate that the model with time-varying parameters obtained by solely assimilating streamflow data performed better in streamflow simulation than the one with constant parameters, but the improvement was small. The model simulation improved considerably when the time-varying parameters were estimated by adding *ET* data into assimilation with streamflow. In addition, scheme 2 showed higher NSE_Q and NSE_{ET} than scheme 1 in 109 and 173 catchments (Fig. 7), respectively, where the NSE_{ET} values increased from 0.06 to 0.7, especially in humid areas. Besides, the model simulation performance with time invariant and time-varying (scheme 2) model parameters for humid and arid regions is presented in Fig. 8. It can be illustrated that the climate conditions influenced the model simulation. On average, the streamflow

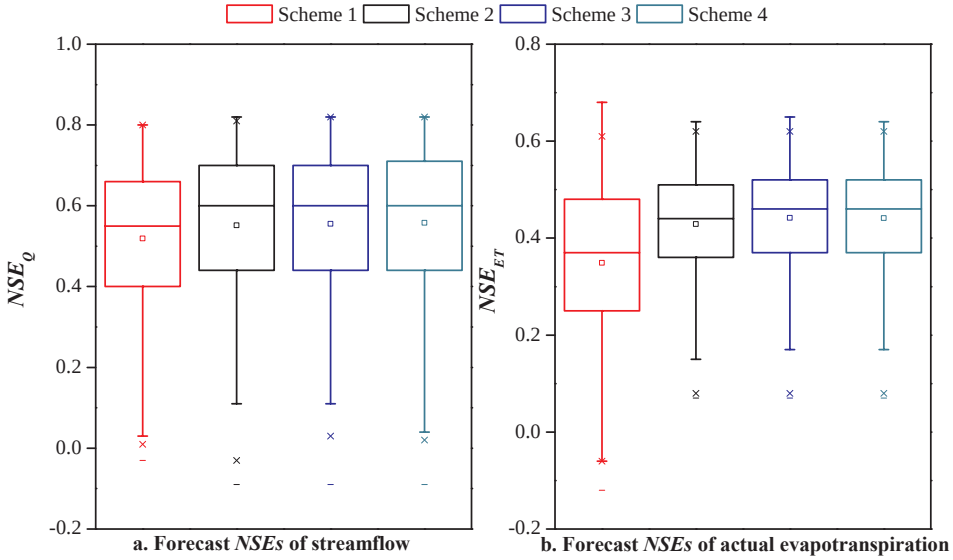

Fig. 5. The forecast Nash-Sutcliffe efficiency coefficients of streamflow and actual evapotranspiration for scheme 1 (red box), scheme 2 (black box), scheme 3 (blue box) and scheme 4 (green box). (For interpretation of the references to colour in this figure legend, the reader is referred to the web version of this article.)

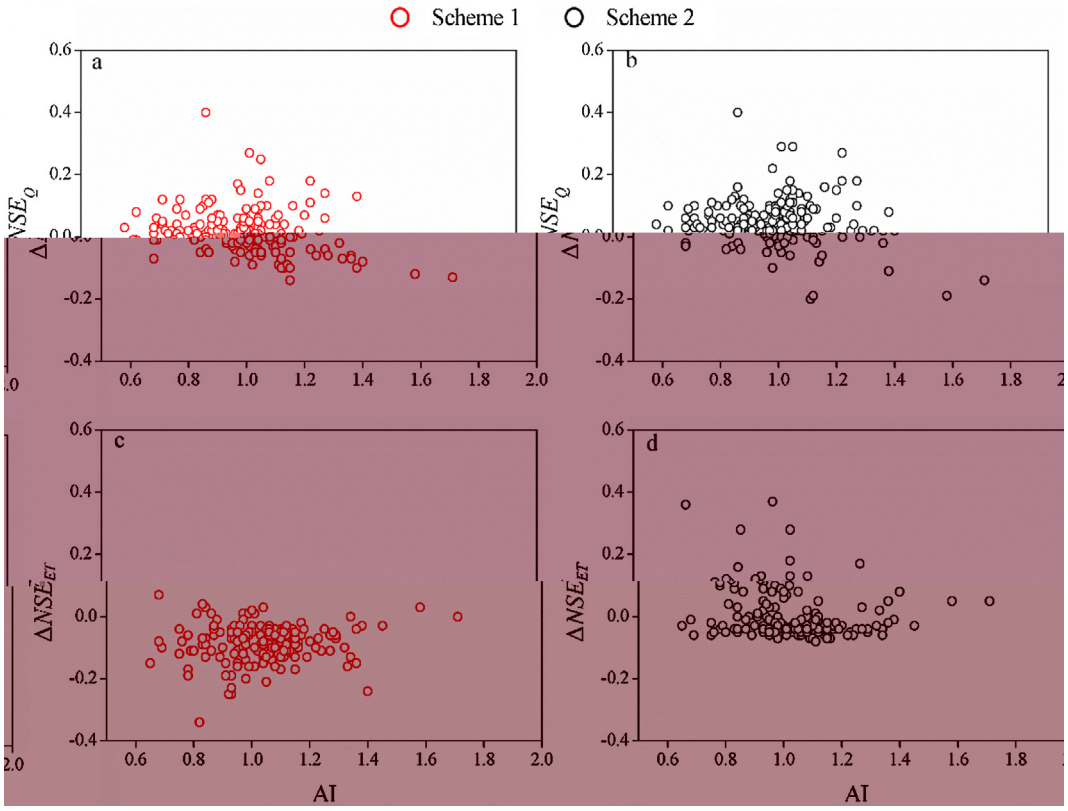

Fig. 6. The correlogram of the aridity index and difference values of the forecast Nash-Sutcliffe efficiency coefficients of streamflow (ΔNSE_Q) and actual evapotranspiration (ΔNSE_{ET}) between scheme 1 (red), scheme 2 (black) and the time invariant scheme. (For interpretation of the references to colour in this figure legend, the reader is referred to the web version of this article.)

simulation was better in humid catchments than in arid catchments because of the applicability of the adopted hydrological model, while the reverse conclusion was observed for the *ET* simulations.

Overall, the time-varying model parameters obtained by adding *ET* data into assimilation with streamflow led to a significant enhancement in deterministic streamflow and *ET* simulation, than the model parameters based on solely assimilating streamflow and time invariant approaches. The streamflow simulation was better in humid catchments than in arid catchments for all the parameter schemes, while the reverse conclusion was observed for the *ET* simulations.

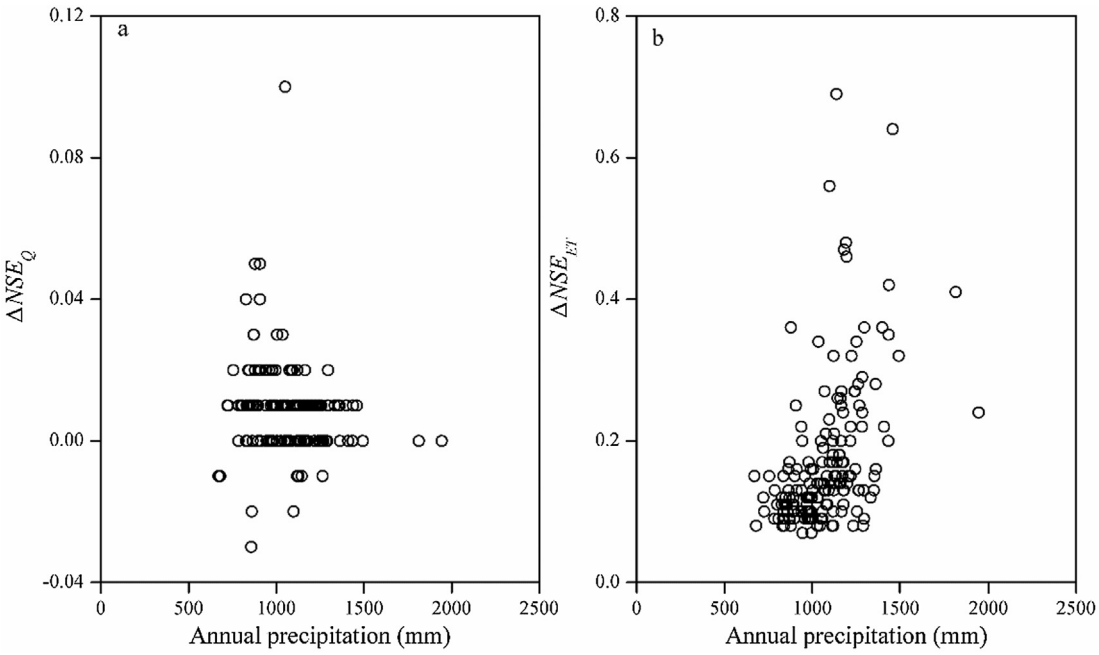

Fig. 7. The correlogram of the annual precipitation and difference values of Nash-Sutcliffe efficiency coefficients of streamflow (left) and actual evapotranspiration (right) between schemes 1 and 2.

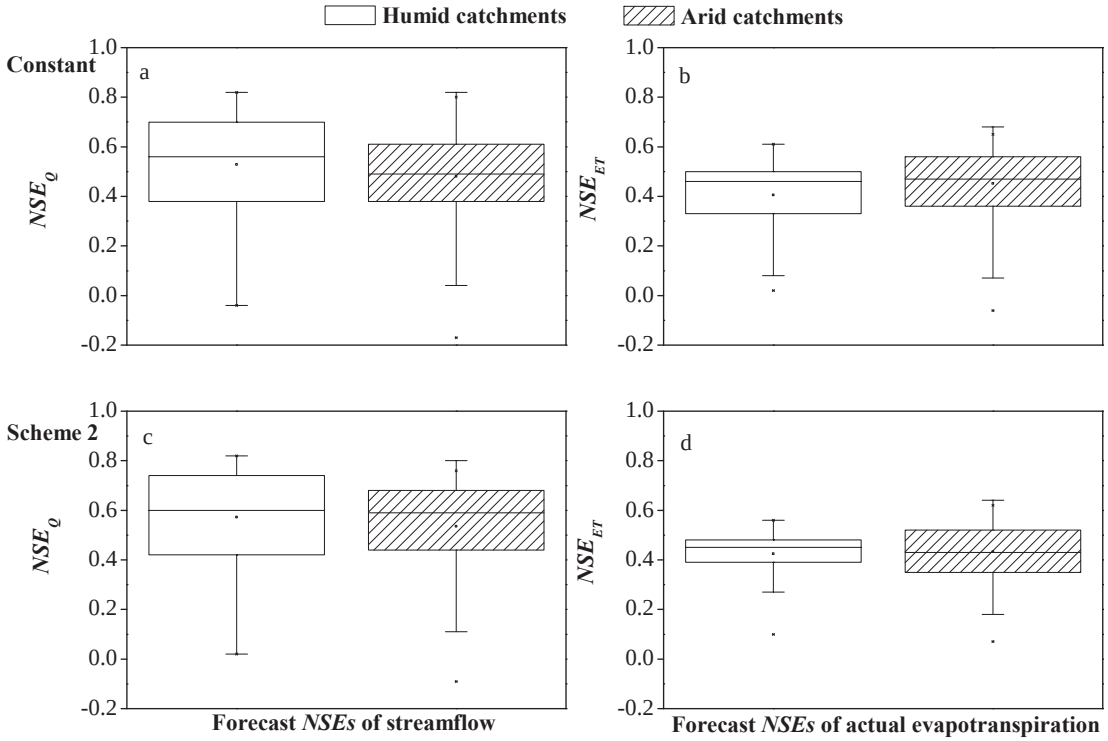

Fig. 8. The Nash-Sutcliffe efficiency coefficients of streamflow and actual evapotranspiration for constant parameters (a, b) and scheme 2 (c, d) for humid catchments (blank box) and arid catchments (shadowy box).

4.3. The effects of joint assimilation on the correlations between parameters

All the four data assimilation schemes had excellent performances in streamflow simulation, and the three joint assimilation schemes showed an improved accuracy in *ET* simulation. To further examine whether the four schemes were reasonable, the correlations between model parameters were compared.

The model parameters were expected to be only weakly correlated, otherwise a change in one parameter may cause other parameters to change, making the optimal values of parameters not unique. Therefore, it was not necessary to set multiple parameters as if they were highly correlated. Fig. 9 presents the Pearson correlation coefficients (R) between C and SC and their absolute values ($|R|$) for the four schemes, given separately for each catchment. On average, C was positively correlated with SC for scheme 1. The number of positively and negatively correlated catchments for the other three schemes was approximately equal. From Fig. 9b, it can be seen that the sole assimilation of streamflow led to the highest correlation between C and SC, with $|R|$ in 110 catchments over 0.3. The three joint assimilation schemes showed weaker correlations, with only 6, 13 and 12 catchments with $|R|$ larger than 0.3, respectively. The medians and mean correlation coefficients between C and SC were around 0.1 and 0.12 for scheme 2, and around 0.12 and 0.13 for scheme 3 and scheme 4. Scheme 2 showed weaker correlation between parameters than scheme 1 in 151 catchments, where the absolute values of R decreased from 0.01 to 0.7, especially in humid areas (Fig. 10). In general, the joint assimilation

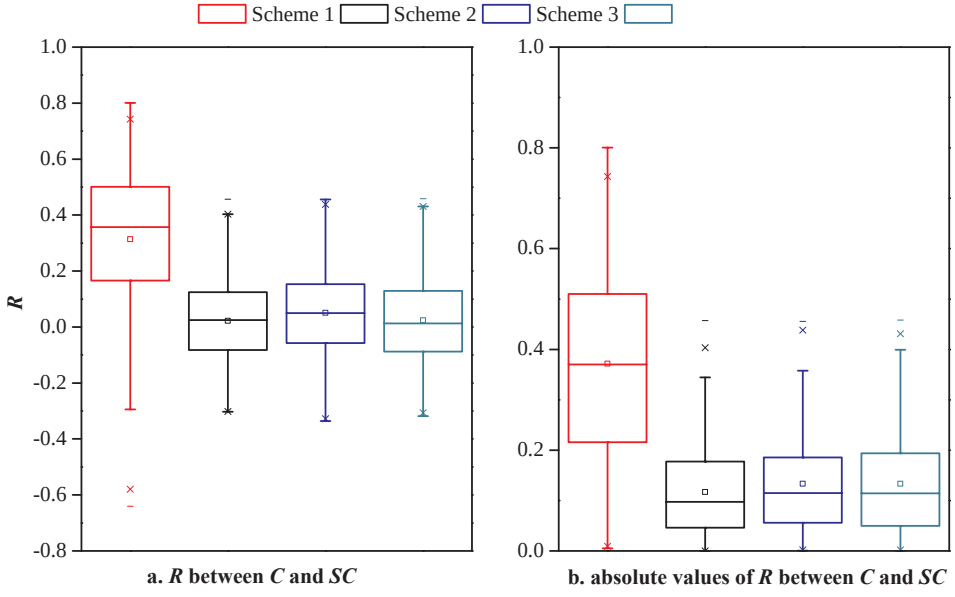

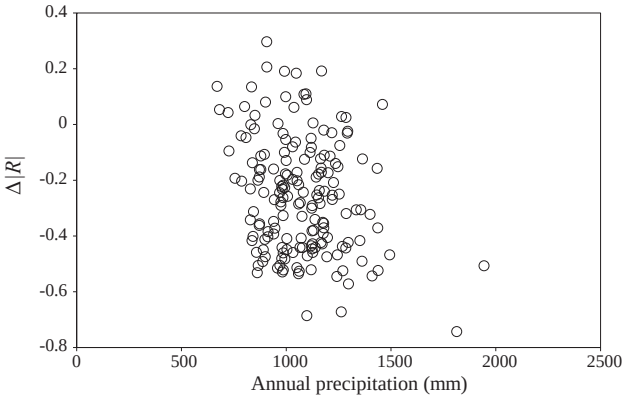

Fig. 10. The correlogram of annual precipitation and absolute difference values of correlation coefficients between scheme 2 and scheme 1. A negative ΔR value indicates weaker correlation between parameters in scheme 2.

schemes could reduce the correlation between model parameters, and scheme 2 was able to generate more applicable parameter series.

5. Conclusions

The EnKF method was used to assimilate streamflow and *ET* data into a monthly water balance model to identify time-varying parameters. Four data assimilation schemes were designed in this study, including: (1) sole assimilation of streamflow to update both parameters, (2) joint assimilation of streamflow and *ET* to update both parameters, (3) sole assimilation of *ET* first to update parameter *C*, and then subsequently joint assimilation of streamflow and *ET* to update parameter *SC*, and (4) sole assimilation of *ET* to update parameter *C*, and then sole assimilation of streamflow to update parameter *SC*. Based on the results of the synthetic experiment and case study in 173 catchments in USA, we drew the following conclusions.

(1) The time-varying model parameter estimation framework using the EnKF method was able to identify the temporal variation of the model parameters, and to produce accurate 95% predictive bounds for streamflow. The estimation of parameter *C* (measuring evapotranspiration) can be improved by assimilating *ET* observations into the model. The time-varying model parameters obtained by adding *ET* data into assimilation with streamflow led to a significant enhancement in deterministic streamflow and *ET* simulation, than the model parameters based on solely assimilating streamflow and time invariant approaches.
(2) For the three joint assimilation schemes, the deterministic model performances were similar, while the ensemble predictions were more reliable in scheme 2. The joint assimilation of streamflow and *ET* to update both parameters in one step, i.e., scheme 2, outperformed the other two in parameter *SC* estimation and reliable ensemble prediction.
(3) The ability to enhance *ET* simulation accuracy was better in humid catchments. with *NSE* values increasing by around 0.7 in some humid areas. The ability to reduce correlation between parameters was also better in humid catchments, with *R* values decreasing by more than 0.7.

Because our research demonstrates the best scheme for estimating time-varying parameters, future work will be focused on the relationship between parameter variations and input observations or land use changes.

Acknowledgements

This study was supported by the National Key Research and Development Program (2016YFC0400907), the Innovative Research Groups of the Natural Science Foundation of Hubei, China (2017CFA015) and the National Natural Science Foundation of China (51579180). Sincere gratitude is extended to the editor and anonymous reviewers for their professional comments and corrections, which greatly improved the presentation of the paper.

References

Abbaszadeh, P., Moradkhani, H., Yan, H., 2018. Enhancing hydrologic data assimilation by evolutionary Particle Filter and Markov Chain Monte Carlo. Adv. Water Resour. 111, 192–204. https://doi.org/10.1016/j.advwatres.2017.11.011.
Brigode, P., Oudin, L., Perrin, C., 2013. Hydrological model parameter instability: a source of additional uncertainty in estimating the hydrological impacts of climate change? J. Hydrol. 476, 410–425. https://doi.org/10.1016/j.jhydrol.2012.11.012.
Brown, A.E., Zhang, L., McMahon, T.A., Western, A.W., Vertessy, R.A., 2005. A review of paired catchment studies for determining changes in water yield resulting from alterations in vegetation. J. Hydrol. 310 (1–4), 28–61. https://doi.org/10.1016/j.jhydrol.2004.12.010.
Budyko, M.I., 1974. Climate and Life. Academic, New York.
Camporese, M., Paniconi, C., Putti, M., Salandin, P., 2009. Ensemble Kalman filter data assimilation for a process-based catchment scale model of surface and subsurface flow. Water Resour. Res. 45. https://doi.org/10.1029/2008wr007031.
Clark, M.P., et al., 2008. Hydrological data assimilation with the ensemble Kalman filter: use of streamflow observations to update states in a distributed hydrological model. Adv. Water Resour. 31 (10), 1309–1324. https://doi.org/10.1016/j.advwatres.2008.06.005.
de Vos, N.J., Rientjes, T.H.M., Gupta, H.V., 2010. Diagnostic evaluation of conceptual rainfall-runoff models using temporal clustering. Hydrol. Process. 24 (20), 2840–2850. https://doi.org/10.1002/hyp.7698.
DeChant, C.M., Moradkhani, H., 2012. Examining the effectiveness and robustness of sequential data assimilation methods for quantification of uncertainty in hydrologic forecasting. Water Resour. Res. 48. https://doi.org/10.1029/2011wr011011.
Deng, C., Liu, P., Guo, S., Li, Z., Wang, D., 2016. Identification of hydrological model parameter variation using ensemble Kalman filter. Hydrol. Earth Syst. Sci. 20 (12), 4949–4961. https://doi.org/10.5194/hess-20-4949-2016.
Deng, C., Liu, P., Guo, S., Wang, H., Wang, D., 2015. Estimation of nonfluctuating reservoir inflow from water level observations using methods based on flow continuity. J. Hydrol. 529, 1198–1210. https://doi.org/10.1016/j.jhydrol.2015.09.037.
Deng, C., Liu, P., Wang, D.B., Wang, W.G., 2018. Temporal variation and scaling of parameters for a monthly hydrologic model. J. Hydrol. 558, 290–300. https://doi.org/10.1016/j.jhydrol.2018.01.049.
Dong, Q., Zhan, C., Wang, H., Wang, F., Zhu, M., 2016. A review on evapotranspiration data assimilation based on hydrological models. J. Geog. Sci. 26 (2), 230–242. https://doi.org/10.1007/s11442-016-1265-4.
Duan, Q., et al., 2006. Model Parameter Estimation Experiment (MOPEX): an overview of science strategy and major results from the second and third workshops. J. Hydrol. 320 (1–2), 3–17. https://doi.org/10.1016/j.jhydrol.2005.07.031.
Evensen, G., 1994. Sequential data assimilation with a nonlinear quasi-geostrophic model using Monte Carlo methods to forecast error statistics. J. Geophys. Res.-Oceans 99 (C5), 10143–10162. https://doi.org/10.1029/94jc00572.
Evensen, G., 2004. Sampling strategies and square root analysis schemes for the EnKF. Ocean Dyn. 54 (6), 539–560. https://doi.org/10.1007/s10236-004-0099-2.
Feng, M., et al., 2017. Deriving adaptive operating rules of hydropower reservoirs using time-varying parameters generated by the EnKF. Water Resour. Res. 53 (8), 6885–6907. https://doi.org/10.1002/2016wr020180.
Gharari, S., Hrachowitz, M., Fenicia, F., Savenije, H.H.G., 2013. An approach to identify time consistent model parameters: sub-period calibration. Hydrol. Earth Syst. Sci. 17 (1), 149–161. https://doi.org/10.5194/hess-17-149-2013.
Guo, S.L., Wang, J.X., Xiong, L.H., Ying, A.W., Li, D.F., 2002. A macro-scale and semi-distributed monthly water balance model to predict climate change impacts in China. J. Hydrol. 268 (1–4), 1–15. https://doi.org/10.1016/s0022-1694(02)00075-6.
Jeremiah, E., Marshall, L., Sisson, S.A., Sharma, A., 2013. Specifying a hierarchical mixture of experts for hydrologic modeling: gating function variable selection. Water Resour. Res. 49 (5), 2926–2939.
Jung, M., et al., 2010. Recent decline in the global land evapotranspiration trend due to limited moisture supply. Nature 467 (7318), 951–954. https://doi.org/10.1038/nature09396.
Kalma, J.D., McVicar, T.R., McCabe, M.F., 2008. Estimating land surface evaporation: a review of methods ssing remotely sensed surface temperature data. Surv. Geophys. 29 (4–5), 421–469. https://doi.org/10.1007/s10712-008-9037-z.
Legesse, D., Vallet-Coulomb, C., Gasse, F., 2003. Hydrological response of a catchment to climate and land use changes in Tropical Africa: case study South Central Ethiopia. J. Hydrol. 275 (1–2), 67–85. https://doi.org/10.1016/s0022-1694(03)00019-2.
Leisenring, M., Moradkhani, H., 2012. Analyzing the uncertainty of suspended sediment load prediction using sequential data assimilation. J. Hydrol. 468, 268–282. https://doi.org/10.1016/j.jhydrol.2012.08.049.
Marshall, L., Sharma, A., Nott, D., 2006. Modeling the catchment via mixtures: issues of model specification and validation. Water Resour. Res. 42 (11), W11409. https://doi.org/10.1029/2005wr004613.
Merz, R., Parajka, J., Bloeschl, G., 2011. Time stability of catchment model parameters: implications for climate impact analyses. Water Resour. Res. 47 (2), W02531. https://doi.org/10.1029/2010wr009505.

Mitchell, H.L., Houtekamer, P.L., 2000. An adaptive ensemble Kalman filter. Mon. Weather Rev. 128 (2), 416–433.
Montzka, C., Pauwels, V.R.N., Franssen, H.-J.H., Han, X., Vereecken, H., 2012. Multivariate and multiscale data assimilation in terrestrial systems: a review. Sensors 12 (12), 16291–16333. https://doi.org/10.3390/s121216291.
Moradkhani, H., DeChant, C.M., Sorooshian, S., 2012. Evolution of ensemble data assimilation for uncertainty quantification using the particle filter-Markov chain Monte Carlo method. Water Resour. Res. 48. https://doi.org/10.1029/2012wr012144.
Moradkhani, H., Sorooshian, S., Gupta, H.V., Houser, P.R., 2005. Dual state-parameter estimation of hydrological models using ensemble Kalman filter. Adv. Water Resour. 28 (2), 135–147. https://doi.org/10.1016/j.advwatres.2004.09.002.
Nash, J.E., Sutcliffe, J.V., 1970. River flow forecasting through conceptual models part I: a discussion of principles. J. Hydrol. 10 (3), 282–290. https://doi.org/10.1016/0022-1694(70)90255-6.
Pathiraja, S., Anghileri, D., Burlando, P., Sharma, A., Marshall, L., Moradkhani, H., 2018. Insights on the impact of systematic model errors on data assimilation performance in changing catchments. Adv. Water Resour. https://doi.org/10.1016/j.advwatres.2017.12.006.
Pathiraja, S., Anghileri, D., Burlando, P., Sharma, A., Marshall, L., Moradkhani, H., 2017. Time varying parameter models for catchments with land use change: the importance of model structure. Hydrol. Earth Syst. Sci. Discuss. https://doi.org/10.5194/hess-2017-382.
Pathiraja, S., Marshall, L., Sharma, A., Moradkhani, H., 2016a. Detecting non-stationary hydrologic model parameters in a paired catchment system using data assimilation. Adv. Water Resour. 94, 103–119. https://doi.org/10.1016/j.advwatres.2016.04.021.
Pathiraja, S., Marshall, L., Sharma, A., Moradkhani, H., 2016b. Hydrologic modeling in dynamic catchments: a data assimilation approach. Water Resour. Res. 52 (5), 3350–3372. https://doi.org/10.1002/2015wr017192.
Patil, S.D., Stieglitz, M., 2015. Comparing spatial and temporal transferability of hydrological model parameters. J. Hydrol. 525, 409–417. https://doi.org/10.1016/j.jhydrol.2015.04.003.
Priestley, C.H.B., Taylor, R.J., 1972. On the assessment of surface heat flux and evaporation using large-scale parameters. Mon. Weather Rev. 100, 81–92.
Qin, C., et al., 2008. Integrating remote sensing information into a distributed hydrological model for improving water budget predictions in large-scale basins through data assimilation. Sensors 8 (7), 4441–4465. https://doi.org/10.3390/s8074441.
Renard, B., Kavetski, D., Kuczera, G., Thyer, M., Franks, S.W., 2010. Understanding predictive uncertainty in hydrologic modeling: The challenge of identifying input and structural errors. Water Resour. Res. 46. https://doi.org/10.1029/2009wr008328.
Schuurmans, J.M., Troch, P.A., Veldhuizen, A.A., Bastiaanssen, W.G.M., Bierkens, M.F.P., 2003. Assimilation of remotely sensed latent heat flux in a distributed hydrological model. Adv. Water Resour. 26 (2), 151–159. https://doi.org/10.1016/s0309-1708(02)00089-1.
Seibert, J., McDonnell, J.J., Woodsmith, R.D., 2010. Effects of wildfire on catchment runoff response: a modelling approach to detect changes in snow-dominated forested catchments. Hydrol. Res. 41 (5), 378–390. https://doi.org/10.2166/nh.2010.036.
Shi, Y., Davis, K.J., Zhang, F., Duffy, C.J., Yu, X., 2015. Parameter estimation of a physically-based land surface hydrologic model using an ensemble Kalman filter: a multivariate real-data experiment. Adv. Water Resour. 83, 421–427. https://doi.org/10.1016/j.advwatres.2015.06.009.
Smith, P.J., Beven, K.J., Tawn, J.A., 2008. Detection of structural inadequacy in process-based hydrological models: a particle-filtering approach. Water Resour. Res. 44 (1). https://doi.org/10.1029/2006wr005205.
Snyder, C., Zhang, F.Q., 2003. Assimilation of simulated Doppler radar observations with an ensemble Kalman filter. Mon. Weather Rev. 131 (8), 1663–1677. https://doi.org/10.1175//2555.1.
Thirel, G., et al., 2015. Hydrology under change: an evaluation protocol to investigate how hydrological models deal with changing catchments. Hydrol. Sci. J. 60 (7–8), 1184–1199. https://doi.org/10.1080/02626667.2014.967248.
Vaze, J., et al., 2010. Climate non-stationarity – Validity of calibrated rainfall-runoff models for use in climate change studies. J. Hydrol. 394 (3–4), 447–457. https://doi.org/10.1016/j.jhydrol.2010.09.018.
Vrugt, J.A., ter Braak, C.J.F., Diks, C.G.H., Schoups, G., 2013. Hydrologic data assimilation using particle Markov chain Monte Carlo simulation: theory, concepts and applications. Adv. Water Resour. 51, 457–478. https://doi.org/10.1016/j.advwatres.2012.04.002.
Wagener, T., McIntyre, N., Lees, M.J., Wheater, H.S., Gupta, H.V., 2003. Towards reduced uncertainty in conceptual rainfall-runoff modelling: dynamic identifiability analysis. Hydrol. Process. 17 (2), 455–476. https://doi.org/10.1002/hyp.1135.
Wang, D., Chen, Y., Cai, X., 2009. State and parameter estimation of hydrologic models using the constrained ensemble Kalman filter. Water Resour. Res. 45 (11), W11416. https://doi.org/10.1029/2008wr007401.
Westra, S., Thyer, M., Leonard, M., Kavetski, D., Lambert, M., 2014. A strategy for diagnosing and interpreting hydrological model nonstationarity. Water Resour. Res. 50 (6), 5090–5113. https://doi.org/10.1002/2013wr014719.
Xiong, L., Guo, S., 2012. Appraisal of Budyko formula in calculating long-term water balance in humid watersheds of southern China. Hydrol. Process. 26 (9), 1370–1378. https://doi.org/10.1002/hyp.8273.
Xiong, L.H., Guo, S.L., 1999. A two-parameter monthly water balance model and its application. J. Hydrol. 216 (1–2), 111–123. https://doi.org/10.1016/s0022-1694(98)00297-2.
Yan, H., Moradkhani, H., 2016. Combined assimilation of streamflow and satellite soil moisture with the particle filter and geostatistical modeling. Adv. Water Resour. 94, 364–378. https://doi.org/10.1016/j.advwatres.2016.06.002.
Zhang, K., Kimball, J.S., Nemani, R.R., Running, S.W., 2010. A continuous satellite-derived global record of land surface evapotranspiration from 1983 to 2006. Water Resour. Res. 46 (9), W09522. https://doi.org/10.1029/2009wr008800.
Zou, L., Zhan, C., Xia, J., Wang, T., Gippel, C.J., 2017. Implementation of evapotranspiration data assimilation with catchment scale distributed hydrological model via an ensemble Kalman Filter. J. Hydrol. 549, 685–702. https://doi.org/10.1016/j.jhydrol.2017.04.036.